Path-Aware and Structure-Preserving Generation of Synthetically Accessible Molecules

Juhwan Noh [1] **Dae-Woong Jeong** [2] **Kiyoung Kim** [2] **Se-Hui Han** [2] **Moontae Lee** [2 3] **Honglak Lee** [2]
Yousung Jung [1 4]

Abstract

Computational chemistry aims to autonomously design specific molecules with target functionality. Generative frameworks provide useful tools to learn continuous representations of molecules in a latent space. While modelers could optimize chemical properties, many generated molecules are not synthesizable. To design synthetically accessible molecules that preserve main structural motifs of target molecules, we propose a reaction-embedded and structure-conditioned variational autoencoder. As the latent space jointly encodes molecular structures and their reaction routes, our new sampling method that measures the path-informed structural similarity allows us to effectively generate structurally analogous synthesizable molecules. When targeting out-of-domain as well as in-domain seed structures, our model generates structurally and property-wisely similar molecules equipped with well-defined reaction paths. By focusing on the important region in chemical space, we also demonstrate that our model can design new molecules with even higher activity than the seed molecules.

1. Introduction

Discovering new molecules with desired properties is the ultimate task in a wide range of industrial applications including pharmaceutical as well as chemical industry, but the conventional trial-and-error type of processes are generally slow and resource-demanding. The main challenge here is the nearly infinite chemical space to explore, making it practically infeasible to exhaustively search through the all relevant molecular space. While expert intuitions have been successful to guide the search traditionally, automating and further accelerating these processes is critical to meet different industrial needs in a timely manner.

Data-driven approaches can dramatically facilitate the molecular discovery by utilizing available chemical knowledge extracted from data, enabling automated and fast exploration of the chemical space (Pollice et al., 2021). Indeed, there have been a significant surge in using machine learning for molecular design in recent years, and there are many excellent reviews that offer extensive summaries and perspectives on the subject (Zunger, 2018; Sanchez-Lengeling & Aspuru-Guzik, 2018; Elton et al., 2019). Among different such approaches, generative model is particularly promising strategy of molecular design which can generate new molecules with desired properties leveraging the learned chemical distribution (Putin et al., 2018; Gómez-Bombarelli et al., 2018; Hong et al., 2019; Méndez-Lucio et al., 2020; Maziarka et al., 2020). Many successful proof-of-concept demonstrations have been reported for molecular property optimizations, however, as discussed in Gottipati et al. (2020), many of the newly generated molecules have practical challenges in actual lab synthesis, posing a large gap between the theoretical predictions and experimental validations.

To overcome this synthesizability bottleneck, several methods have been proposed mainly in two different directions: synthesizability metric-based heuristics or retrosynthesis reaction planning. The first approach utilizes synthesizability metrics either designed by analyzing the occurrence of molecular fragments (Ertl & Schuffenhauer, 2009; Voršilák et al., 2020) or learned from reactions (Boda et al., 2007; Huang et al., 2011; Gao & Coley, 2020; Thakkar et al., 2021). But, these metric-based approaches suggest the synthesizability based on the correlation analyses without considering the actual routes to synthesis or are inherently limited by the underlying dataset or models used for learning metrics. Thus, high synthesizability scores could not directly transfer to practical use. The second retrosynthetic

[1]Department of Chemical and Biomolecular Engineering (BK21 four), Korea Advanced Institute of Science and Technology, Republic of Korea [2]LG AI Research, Republic of Korea [3]Department of Information and Decision Sciences, University of Illinois Chicago, USA [4]Graduate School of Artificial Intelligence, Korea Advanced Institute of Science and Technology, Republic of Korea. Correspondence to: Yousung Jung <ysjn@kaist.ac.kr>.

Proceedings of the 39^{th} International Conference on Machine Learning, Baltimore, Maryland, USA, PMLR 162, 2022.

approach is based on learning chemical reactions in an inverse manner and attempts to predict reactant molecules from the product information, and thus actual synthetic pathways and easiness can be evaluated (Segler & Waller, 2017; Coley et al., 2017; Liu et al., 2017; Segler et al., 2018; Schwaller et al., 2019; Dai et al., 2019; Karpov et al., 2019; Shi et al., 2020; Liu et al., 2020; Schwaller et al., 2020; Duan et al., 2020; Tetko et al., 2020; Sacha et al., 2021; Somnath et al., 2021; Chen & Jung, 2021; Mann & Venkatasubramanian, 2021; Ucak et al., 2022). These methods of predicting synthesizability or retrosynthetic reaction predictions can then be used in conjunction with aforementioned generative models to sequentially design synthesizable molecules with target properties. However, since the property-optimized molecules obtained from conventional generative models have not learned the reaction information, many of those generated target molecules do not have feasible reaction pathways, requiring repeated application of post-hoc retrosynthesis planning tasks until one finds synthesizable active molecules. Thus, those post-hoc processes can be slow and ineffective. One possible solution to this sequential task is to generate synthetically accessible molecules on the fly during the generation step (Section 2).

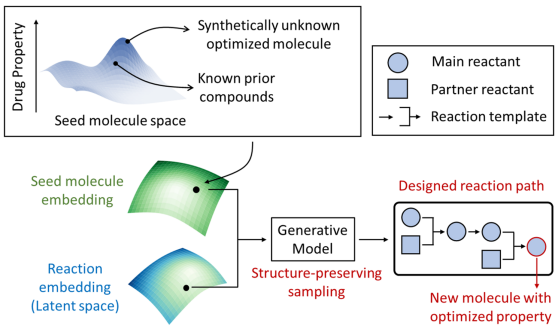

Figure 1. Illustration of the scope of this work for generating structurally conditioned molecules with synthesis pathways. Our model includes two embedding domains: reaction embedding to ensure synthesizability and seed molecule embedding for structure-preserving generation. Seed molecules could be either known prior compounds or virtual molecules whose properties were independently optimized but their synthesizability undetermined.

In this work, we proposed a reaction-embedded structure-conditioned generative model (Kingma & Welling, 2013; Sohn et al., 2015) to seamlessly design synthetically accessible molecules preserving the main structural motifs of seed molecules. To define the scope of the present work as shown in Figure 1, seed molecules here are the molecules that are property-optimized already from a separated molecular design pipeline such as generative models with its synthesizability unknown, and our goal is to generate "seed-like" molecules with their synthesis pathways attached. The seed molecules can also be existing molecules in the market with high activity, and in this case our model would be focusing on the important region of chemical space close to the known active molecules to discover synthetically accessible version with even higher activity. The proposed approach is motivated partly by and consistent with the chemist's usual intuitions on the structure-property relationships, i.e., structures largely determine the properties (Bender & Glen, 2004; Eckert & Bajorath, 2007; Nigam et al., 2021). To this end, the key contributions of this work are:

- We propose a latent variable-driven conditional generative model with variational autoencoder (VAE) that seamlessly incorporate the synthesizability of generated molecules using commercially available compounds into the design pipeline that preserve the structural similarity to the seed compound.
- We demonstrate that a conventional sampling scheme relying on the structural distance of reactants alone is insufficient to generate products after the reaction, and the whole reaction information is required to properly measure the similarity to the seed compound during the generation.
- We show using the out-of-domain dataset that the present model can effectively generate molecules with the proper synthesis pathways and even higher activity by focusing on the important region in chemical space starting from the given seed molecules.

2. Related Work

We here briefly summarize the related previous work to generate molecules with desired property while ensuring synthesizability built into the model. Bradshaw et al. (2019) incorporated the synthesizability into the molecular design by generating a bag of reactants, rather than the target molecules themselves (i.e. MOLECULE CHEF), that are then combined to yield the target product by applying the pretrained template-free forward synthesis model. It successfully demonstrated to generate valid molecules and its reaction path simultaneously, and also shown its applicability for property optimization task, though limited to the use of single step reactions in the generation. The same authors (Bradshaw et al., 2020) subsequently proposed the directed acyclic graph (DAG) representation to generate multi-step molecular synthesis routes with the autoencoder (i.e. DoG-AE/DoG-Gen) and demonstrated the effectiveness of the model for property optimization tasks with multi-step reactions. A similar template-based multi-step reaction generative model was also proposed by Nguyen and Tsuda (2021) where the authors used the reaction tree representation to encode the synthesizability into the model based on junction tree VAE (i.e. JT-VAE, (Jin et al., 2018)). The reinforcement learning (RL)-based forward synthesis planning framework, PGFS (Policy Gradient for Forward Synthesis),

was proposed by Gottipati et al. (2020) to design synthesizable molecules by generating multi-step pathways using the Markov decision process and maximizing the properties based on the reinforcement learning.

Synthesizable molecular designs focusing on the analogs of known active compounds (or seed molecules), the present scope, have also been suggested. Button et al. (2019) proposed the model called *DINGOS* to generate synthetically accessible and structurally similar molecules to the seed compound by selecting the structurally most similar reactants to the seed molecule in the pool and repeatedly applying the known reaction templates. The structural similarity of the reacting molecules, however, does not always mean that the resulting products after applying the reaction templates to them would still be structurally similar to the target seed compound. Indeed, we show below that to find structurally similar synthesizable molecules the synthesis pathway information should be learned simultaneously along with the structural similarity to the target seed molecules.

Our work is most similar to some models in Bradshaw et al. (2019; 2020) and Gao et al. (2021) in terms of the model and scopes. Specifically, the retrosynthesis version of MOLECULE CHEF (Bradshaw et al., 2019) and RetroDoG (Bradshaw et al., 2020) were used to generate the synthesizable molecules similar to the target products. However, since the main scopes of Bradshaw et al. (2019; 2020) were the reaction (rather than molecule) embedding into the latent space to ensure the synthesizability of generated compounds, a separate retrosynthetic regressor mapping from the target products to the latent representation of the corresponding reactants were needed to generate desired products or structurally similar products with synthetic pathways. In addition, the earlier model proposed by Bradshaw et al. (2019) was limited to the product searches obtainable from single-step reactions, while the later model, RetroDoG by Bradshaw et al. (2020), showed a few examples of structurally similar synthesizable molecules with multi-step pathways but without demonstrating the full reconstruction results. In contrast, our model explicitly learns the joint distribution for the structure of seed molecules and their multi-step reaction pathways to seamlessly incorporate the similarity and synthesizability into the latent space and generation. Very recently, concurrent to the present work, a conditional generative approach (i.e. SynNet) was proposed for the purpose of generating synthesizable molecules similar to the target compound by using the Markov decision process to encode synthetic pathways (Gao et al., 2021). The model showed an encouraging reconstruction accuracy on the test molecules. While Gao et al. (2021) and our work aim to produce structurally similar synthesizable molecules and were carried out in parallel, the two models differ by how the conditional generation is performed, either directly using Markov decision process or driven by latent variables.

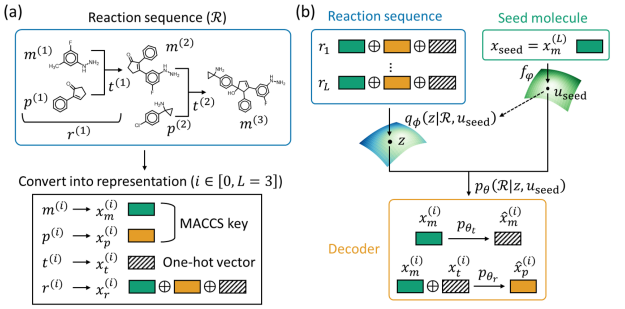

Figure 2. (a) Representation of reaction sequence for two-step reaction (i.e. $n = 2$) as an example. (b) Encoding and decoding scheme of the proposed C-RSVAE with multi-step linear reactions.

3. Methods

3.1. Conditional Reaction Sequence Variational Autoencoder (C-RSVAE)

Reaction Sequence Representation. For notations, let m, p and t be main reactant, partner reactant, and reaction template, respectively, and r be a single-step reaction including m, p and t. The x is used to denote the embedding vectors. We use superscripts in parenthesis to denote the state of the reaction sequence, $\mathcal{R}$, and subscripts to denote the component of $\mathcal{R}$ (i.e. m, p, t and r). For example, $r^{(i)}$ represents i^{th} single-step reaction, and $m^{(i)}$ represents the main reactant in the i^{th} single-step reaction. Similarly, $x_m^{(i)}$ denotes the embedding vector of the main reactant in the i^{th} single-step reaction. Furthermore, we used binary MACCS (**M**olecular **ACC**ess **S**ystem) key for $x_m^{(i)}$ and $x_p^{(i)}$, and used one-hot vector for $x_t^{(i)}$. Also, $x_r^{(i)}$, the embedding vector for the i^{th} single step reaction is defined by concatenating $x_m^{(i)}$, $x_p^{(i)}$ and $x_t^{(i)}$. (i.e. $x_r^{(i)} = x_m^{(i)} \oplus x_p^{(i)} \oplus x_t^{(i)}$). The embedding vector of the seed molecule is denoted as x_{seed} (Figure 2a).

Based on these notations, $\mathcal{R}$ with n single-step reactions is represented by $\mathcal{R} = [r^{(0)}, r^{(1)}, ..., r^{(n)}, r^{(n+1=L)}]$. In this reaction sequence, $m^{(i+1)}$ is same as the product of $r^{(i)}$. The $i = 0$ describes the initial state (i.e. start of reaction), and $i = n + 1 = L$ describes the final state (i.e. end of reaction) of the given reaction sequence. Thus, for the initial state, we set $x_m^{(0)}$ as zero, $x_p^{(0)}$ as $x_m^{(1)}$ and $x_t^{(0)}$ as the start of the reaction token. For the final state, we set $x_p^{(L)}$ as zero and $x_t^{(L)}$ as the end of the reaction token.

Model Architecture. Our model is built on conditional VAE as illustrated in Figure 2b where GRU (Cho et al., 2014) is used to handle sequential data. For notations, let u_{seed} and z be the encoded feature vector of seed molecule and the latent vector of $\mathcal{R}$ conditioned with u_{seed}. Also, the predicted output obtained from the decoder is denoted as $\hat{x}$. For notations of model, let $f_\varphi(x_{\text{seed}})$ be seed molecule

encoder, $q_\phi(z|\mathcal{R}, u_{\text{seed}})$ be reaction sequence encoder and $p_\theta(\mathcal{R}|z, u_{\text{seed}})$ be decoder. Here, φ, ϕ and θ are learnable model parameters. Also, we denote $F(\cdot)$ as a multilayer perceptron (MLP). The proposed model was implemented with Pytorch (Paszke et al., 2019) (see Appendix A for all the other implementation details).

Prior to encoding of the $\mathcal{R}$, x_{seed} is encoded to u_{seed} through the f_φ which is an MLP (i.e. $u_{\text{seed}} = f_\varphi(x_{\text{seed}})$). Next, z is sampled from Gaussian distribution whose mean (μ) and standard deviation (σ) used for reparametrization trick (Kingma & Welling, 2013) are defined as:

$$[\mu, \sigma] = F_h(\text{BiGRU}([x_r^{(1)}, x_r^{(2)}, ..., x_r^{(L)}]|u_{\text{seed}})) \quad (1)$$

where BiGRU is bi-directional GRU (Cho et al., 2014; Schuster & Paliwal, 1997).

Decoding of z with the given condition of u_{seed} through $p_\theta(\mathcal{R}|z, u_{\text{seed}})$ consists of two sub-modules motivated from (Gottipati et al., 2020): reaction template predictor (p_{θ_t}) and reactant predictor (p_{θ_r}) with learnable parameters θ_t and θ_r. p_{θ_t} predicts $x_t^{(i)}$ corresponding to $x_m^{(i)}$, and p_{θ_r} predicts $x_m^{(1)} = x_p^{(0)}$ and $x_p^{(i>0)}$ corresponding to $x_m^{(i>0)}$ and $x_t^{(i>0)}$. Thus, the predicted output of each model is defined as:

$$\begin{aligned}\hat{x}_t^{(j)} &\sim p_{\theta_t}(m^{(j)}|z, u_{\text{seed}}) \\ &= \text{Softmax}[F_t(\text{GRU}(x_m^{(j)}|z, u_{\text{seed}}))] \quad (2)\\ \hat{x}_p^{(k)} &\sim p_{\theta_r}(m^{(k)}, t^{(k)}|z, u_{\text{seed}}) \\ &= \text{Softmax}[F_t(\text{GRU}([x_m^{(k)} \oplus x_t^{(k)}]|z, u_{\text{seed}}))] \quad (3)\end{aligned}$$

where $j \in [1, L]$ and $k \in [0, L-1]$. We only utilize the trained decoder for sampling new molecules with the target seed molecules (see section 3.2).

Objective Function. We define the loss function $\mathcal{L}(\mathcal{R}, u_{\text{seed}})$ using the variational lower bound of the log-probability of a reaction sequence and seed molecule $(\mathcal{R}, u_{\text{seed}})$ as follows:

$$\begin{aligned}\log p(\mathcal{R}, u_{\text{seed}}) &\geq \mathbb{E}_z[\log(\frac{p_\theta(\mathcal{R}|u_{\text{seed}}, z)p(u_{\text{seed}})p(z)}{q_\phi(z|\mathcal{R}, u_{\text{seed}})})] \\ &= \mathbb{E}_z[\log p_\theta(\mathcal{R}|u_{\text{seed}}, z)] + \log p(u_{\text{seed}}) \\ &\quad - \mathcal{L}_{\text{KL}}(q_\phi(z|\mathcal{R}, u_{\text{seed}}) \parallel p(z)) \\ &= -\mathcal{L}(\mathcal{R}, u_{\text{seed}}) \quad (4)\end{aligned}$$

where $z \sim q_\phi(z|\mathcal{R}, u_{\text{seed}})$. $q_\phi(z|\mathcal{R}, u_{\text{seed}})$ is a variational posterior, and regularized with the prior of z, $p(z)$ (i.e. Gaussian with zero-mean and unit-variance) through the KL-divergence term (i.e. $\mathcal{L}_{\text{KL}}$). $p(u_{\text{seed}})$is the prior of feature vector encoding the seed molecule, but it is constant in terms of optimizing the model parameters (i.e. it is not parameterized with any learnable parameters). For reconstruction loss term, $\mathbb{E}_z[-\log p_\theta(\mathcal{R}|z, u_{\text{seed}})]$ is modeled by the summation of loss function predicting the reaction templates (i.e. cross entropy loss, CE) and reactant molecules (i.e. binary cross entropy loss, BCE) since we independently predict the reaction templates and reactants through p_{θ_t} and p_{θ_r}. Thus, $\mathcal{L}(\mathcal{R}, u_{\text{seed}})$ with N reaction sequence data existing in mini-batch is defined as:

$$\begin{aligned}\mathcal{L}(\mathcal{R}, u_{\text{seed}}) = \frac{1}{N}\sum_{i=1}^{N}[\frac{1}{L}\sum_{j=1}^{L}\alpha\text{CE}(x_{t,i}^{(j)}, \hat{x}_{t,i}^{(j)}) \\ + \frac{1}{L}\sum_{k=0}^{L-1}\text{BCE}(x_{p,i}^{(k)}, \hat{x}_{p,i}^{(k)}) + \beta\mathcal{L}_{\text{KL},i}] \quad (5)\end{aligned}$$

where i is index of data-point existing in mini-batch. α and β are hyperparameters for balancing between reconstruction and KL-divergence term. Since our model considers two independent trainable parameters for decoder, we empirically introduced α (see also Appendix B). We considered mask vector for reaction templates available for the given main reactant. Binary cross entropy loss for partner reactant prediction is computed only for the bi-molecular reaction templates.

3.2. Sampling Reactions with Seed Molecules

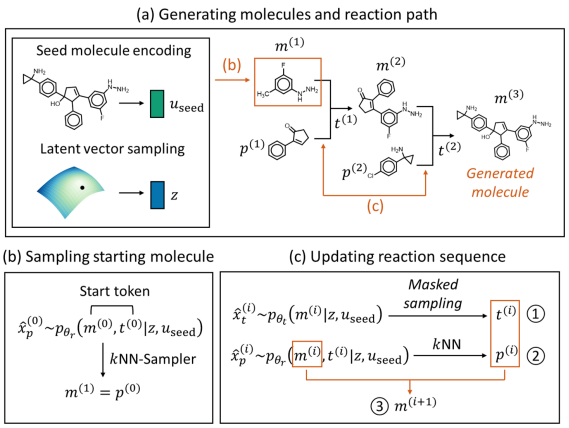

Figure 3. Scheme of molecule generation via the reaction sequence from the trained decoders with seed molecule embedding vector and reaction-embedding latent vector. The generation process is iteratively repeated until the end of reaction token is obtained.

Generating new synthetically accessible molecules from u_{seed} and z sampled from the normal distribution consists of two main steps (Figure 3a): (1) sampling the starting molecules (Figure 3b) and (2) updating reaction sequence (Figure 3c). Since we use the discrete space consisting of a pre-defined set of molecules, sampling of the starting molecule $m^{(1)}$ is expressed as:

$$[m_1^{(1)}, ..., m_k^{(1)}] \sim k\text{NN}_{m\in\mathcal{M}}[H(\hat{x}_m^{(1)}, x_m)] \quad (6)$$

where $\hat{x}_m^{(1)} \sim p_{\theta_r}(m^{(0)}, t^{(0)}|z, u_{\text{seed}})$. $k\text{NN}_{\mathcal{M}}$ is the k-nearest-neighbor-based sampling from the pre-defeind set

$\mathcal{M}$ consisting of starting molecules. For this, we used the Hamming distance, H, between $\hat{x}_m^{(1)}$ and x_m for all m in $\mathcal{M}$. Thus, k similar molecules in $\mathcal{M}$ are selected (i.e. $m_1^{(1)}, ..., m_k^{(1)}$). For an explicit inclusion of the seed molecule information, we further implemented the hybrid sampling approach which additionally measure the similarity between x_{seed} and x_m for all m in $\mathcal{M}$. That is,

$$[m_1^{(1)}, ..., m_k^{(1)}] \sim k\text{NN}_{m\in\mathcal{M}}[(1-\lambda)H(\hat{x}_m^{(1)}, x_m)] + \lambda H(x_{\text{seed}}, x_m)] \quad (7)$$

where λ is a tunable hyperparameter, and we used $\lambda = 0.5$ for all experiments if not explicitly mentioned otherwise (see Appendix F for the effects of changing λ).

Updating of the reaction sequence involves two sub-steps which could be expressed as:

$$\hat{x}_t^{(i)} \sim p_{\theta_t}(m^{(i)}|z, u_{\text{seed}}) \quad (8)$$

$$[p_1^{(i)}, ..., p_k^{(i)}] \sim k\text{NN}_{p\in\mathcal{P}[t^{(i)}]}[H(\hat{x}_p^{(i)}, x_p)] \quad (9)$$

where $\hat{x}_p^{(i)} \sim p_{\theta_r}(m^{(i)}, t^{(i)}|z, u_{\text{seed}})$. The first part is predicting the reaction template $t^{(i)}$ applicable to the current main reactant $m^{(i)}$ with p_{θ_t}. We select $t^{(i)}$ from $\hat{x}_t^{(i)}$ in a greedy manner among the reaction templates matched with $m^{(i)}$. The second part is sampling the partner reactant $p^{(i)}$ using the k-nearest-neighbor-based sampling (i.e. $p_1^{(i)}, ..., p_k^{(i)}$) from the pre-defined set $\mathcal{P}[t^{(i)}]$ consisting of partner molecules matched with the reaction template $t^{(i)}$. Thus, the reaction sequence is updated by applying the reaction template with the sampled molecules (i.e. main reactant and partner reactant). The latter process is applied iteratively until the end of reaction token is predicted through p_{θ_t} or i reaches the pre-defined maximum number of reaction steps, $n_{\max}$ (see Appendix D for additional details).

3.3. Data and Representations

Reaction Database. To construct the reaction database used for training, we used a set of commercially available ∼150,000 molecules obtained from Gottipati et al. (2020) with 58 reaction templates collected from Hartenfeller et al. (2011) relevant to drug discovery. By combinatorically considering the latter set of reactants and reaction templates iteratively, we randomly enumerated total 3 million (M) multi-step chemical reactions (up to three steps). Application of the reaction templates was done with RunReact function implemented in RDKit (Landrum, 2013). Of the 3 M multi-step reactions, 100,000 reactions were then selected randomly to be used as a test set (see Appendix B for additional details).

Representation. All molecules are embedded with a public MACCS key, a binary feature vector with dimension of 166 identifying the existence of the pre-defined molecular fragments as implemented in RDKit (Landrum, 2013). For reaction templates, we distinguished the main reactant position and the partner reactant position for the bi-molecular reaction template, and also included tokens for the start and end of reaction sequence. Thus, the final dimension of reaction template is 116 represented by one-hot encoding.

4. Experiments

4.1. In-Domain Target Seed Recovery

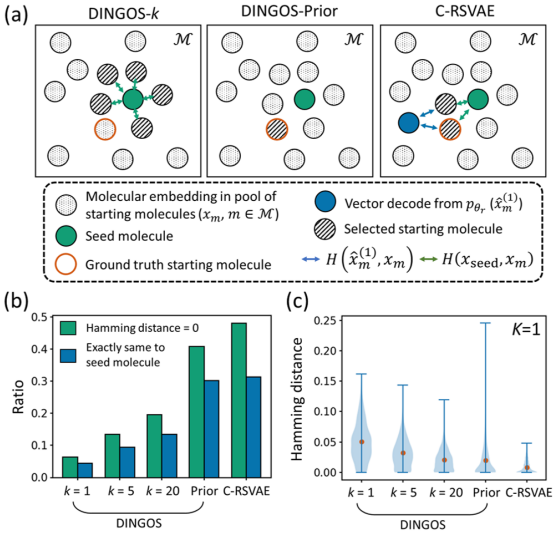

Figure 4. (a) Schematic diagram of DINGOS-k, DINGOS-Prior, and C-RSVAE. (b) The seed molecule recovery ratio with Hamming distance of zero (green) or the identical structure (blue). (c) Distribution of Hamming distance for the top 1 similar molecules where orange circle means the average value of the distribution.

We first consider a toy benchmark in which to investigate the seed molecule recovery for the test set molecules. For that, of the 100,000 multi-step reactions in the test set, we randomly chose 1,000 reactions and used the final product of each multi-step reaction as the seed molecule to be used for benchmarking. The recovery ratio of 1.00 would mean that the generated similar molecules are identical to the seed molecules for all 1,000 products.

We considered five models for comparison as shown in Figure 4a: DINGOS-1, DINGOS-5, DINGOS-20, DINGOS-Prior and C-RSVAE. DINGOS-k (k=1,5,20) selects k most similar main reactants based on H measured in reference to the seed molecule (Button et al., 2019). DINGOS-Prior uses the ground-truth reactant molecules in the test set that lead to the correct seed molecule as the initial main reactants. C-RSVAE is our proposed model which uses the latent vector z randomly sampled from the Normal distribution, with the target seed molecule used as a condition. The overall sampling setup can be found in Appendix D.

The model performance (recovery ratio) and the distribution of the Hamming distance for the most similar generated molecules are summarized in Figure 4b and 4c, respectively. To measure the recovery ratio, we considered a Hamming distance of zero (i.e. the newly generated molecules have the identical type of substructures as found in the target seed molecule). In addition, since it is possible that different molecules can also have the same substructures, we further analyzed whether the generated molecules are indeed identical to the target seed molecule. We note that the reaction sequence reconstruction accuracy of C-RSVAE over all test set data is 98 % by applying the encoder-decoder full pipeline as shown in Figure 2b.

Within the DINGOS-*k*-based approaches, it is observed that the seed molecule recovery ratio increases as more initial molecules (increasing k) are sampled to start the reaction sequence, but DINGOS-Prior, which uses the ground-truth main reactant information, significantly outperforms the other DINGOS-*k* models by 2-7 times. It clearly demonstrates that the use of molecules structurally similar to the target seed molecule as initial main reactant is insufficient to generate the most similar final products after applying the reaction templates. The same trend is observed from the distribution of Hamming distance of the generated molecules relative to the target seed molecule, where choosing the initial main reactants to be structurally most similar to the target seed molecule yields poorer results compared to using structurally less similar molecules but involving correct reaction information.

These results can be compared with C-RSVAE where both structural similarity and reaction sequence information are simultaneously encoded in the latent space. Indeed, C-RSVAE consistently outperforms DINGOS-*k* for all *k* by 2-7 times, comparable to DINGOS-Prior even if our model does not use any additional information on the ground truth reactant as input when generating new molecules as in DINGOS-Prior. Instead, the latter ground truth reactant information is rather embedded in the latent representation of our model via learning the reaction sequence during the training.

4.2. Design of Structure-Preserving Synthesizable Molecules

The main practical application of the proposed C-RSVAE and previous DINGOS is generating new molecules structurally similar to the predefined (usually property-optimized) seed compound, so in this section we demonstrate the model performance by comparing the structural similarity of the generated molecules to the seed target. For this experiment, we randomly sampled 1,000 seed molecules from the test set as in-domain benchmark (not same as seed molecules used in Figure 4) and USPTO registered in year 2016 (USPTO 2016) as out-of-domain benchmark obtained

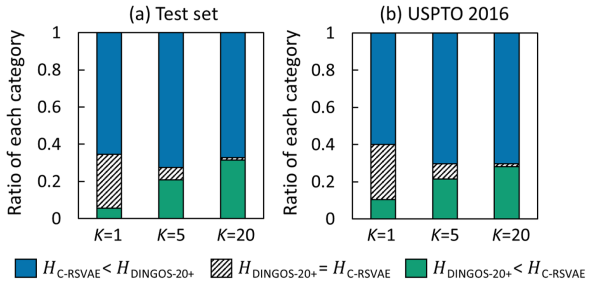

Figure 5. Comparison of Hamming distance for the generated molecules to the seed molecules for C-RSVAE vs. DINGOS-20+. Seed molecules are randomly chosen from (a) test set or (b) USPTO 2016. The Hamming distance for generated molecules is an averaged value over the top K (=1,5,20) similarity-predicted molecules for each seed compound.

from Schwaller et al. (2019). As a baseline, DINGOS-20+ scheme is used which augments DINGOS-20 for more $m^{(1)}$ when the number of reactions sampled is lower than 300 (i.e. 9 % of test set and 44 % of USPTO 2016).

To compare the model performance, we computed the average Hamming distances between the seed and top K (=1, 5, 20) similar structures generated by DINGOS-20+ ($H_{\text{DINGOS-20+}}$) and C-RSVAE ($H_{\text{C-RSVAE}}$). We then counted the number of seed molecules in three categories, $H_{\text{C-RSVAE}} < H_{\text{DINGOS-20+}}$ (blue), $H_{\text{DINGOS-20+}} = H_{\text{C-RSVAE}}$ (dashed pattern) or $H_{\text{DINGOS-20+}} < H_{\text{C-RSVAE}}$ (green). As observed in Figure 5, for both test and USPTO 2016 datasets, C-RSVAE generates molecules more similar to the target seed molecules than DINGOS-20+ for all K's. This result indicates that the generative approach jointly learned with the seed structure and reaction sequence is a more effective way to design structurally-related molecules to the seed compound after the reaction.

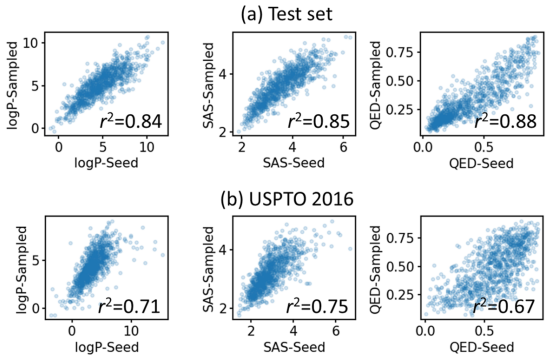

Figure 6. Correlation between the molecular properties (logP, SAS and QED) of the seed molecules and those generated from C-RSVAE. Seed molecules are randomly chosen from (a) test set or (b) USPTO 2016. Top 20 averaged property values are used to compute the coefficient of correlation.

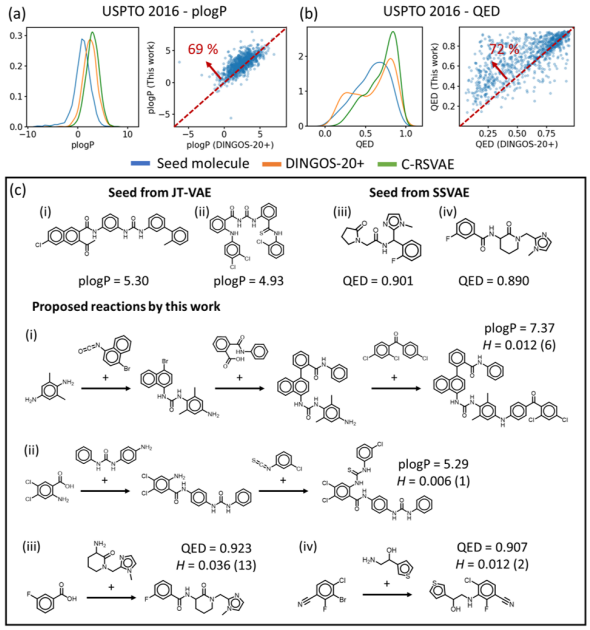

Figure 7. (a-b) Distribution of molecular properties, (a) plogP and (b) QED, for the seed molecules, as well as the comparison between C-RSVAE and DINGOS-20+. We truncate the x-axis near the plateau of the distribution for clarity. The maximum target property within the top 20 similarity predictions are used for generated cases. Seed molecules are randomly chosen from the out-of-domain USPTO 2016. (c) Examples of conditional molecule generation based on the property-optimized seed molecules obtained from (Jin et al., 2018; Kang & Cho, 2018). The listed designed molecules are those with the maximum target property within the top 20 similarity predictions based on the Hamming distance value, with the rank shown in parenthesis: (**i** and **ii**) plogP and (**iii** and **iv**) QED.

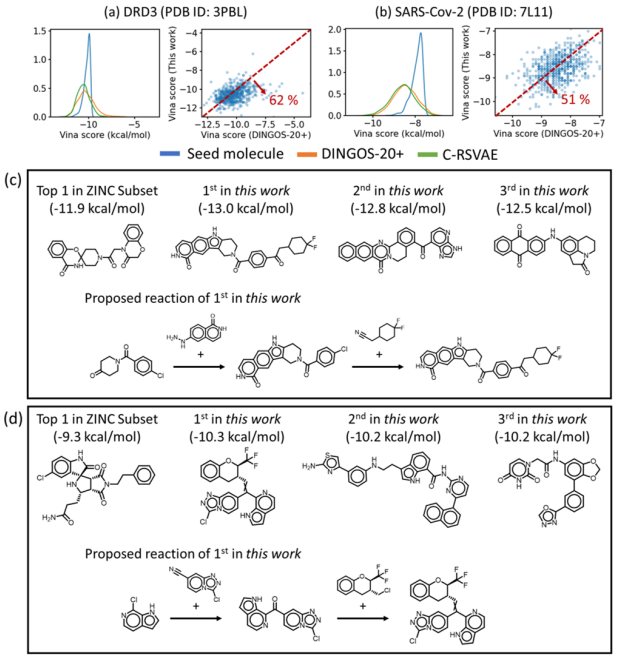

Figure 8. (a-b) Distribution of the docking scores (lower value is better) against (a) DRD3 and (b) M^{pro} of SARS-Cov-2 of seed molecules compared with the generated molecules from C-RSVAE and DINGOS-20+. The minimum target property within the top 20 similarity predictions are used for generated cases. Seed molecules are randomly chosen from the ZINC database. (c-d) Structure of compounds with their reaction paths generated from our model with the top 3 highest docking scores against (c) DRD3 and (d) M^{pro} of SARS-Cov-2.

We next considered the molecular properties of the generated molecules. We considered both the simple properties that can be computed from the RDKit (Landrum, 2013), namely, logP (property related to solubility of molecule), SAS (synthetic accessibility score, (Ertl & Schuffenhauer, 2009)) and QED (drug-likeness), as well as docking scores with Quick Vina 2 (Alhossary et al., 2015) as drug candidates.

The logP, SAS and QED for the generated molecules and their correlations with the target seed molecules are summarized in Figure 6. As desired, a large correlation is seen between the properties of the seed and generated molecules, consistent with the usual structure-property relationship where structurally similar molecules would have similar properties.

As shown in Figure 7a and 7b, there are a significant fraction of seed molecules where the generated structures have even higher properties than the seed molecules. This is due to the fact that the seed molecules used here are not property-optimized toward either of plogP (defined as logP penalized with the synthetic accessibility score and the number of long cycles in (Jin et al., 2018)) or QED but merely taken from the molecule and reaction databases, and so the random sampling of synthesizable molecules around the arbitrary seed compound can give molecules with higher or lower properties. In Figure 7a and 7b, we further analyzed the properties of the generated molecules (the maximum property among the top 20 generated molecules) by C-RSVAE and DINGOS-20+. Molecules with more enhanced properties could be obtained from our approach than DINGOS-20+ due to the utilization of randomly sampled reaction-embedded latent vector that enables the sampling of molecules with relatively diverse property ranges compared to the previous structure-only-constrained design.

Since the main purpose of generating structurally-conditioned synthesizable molecules is to design synthesizable version of property-optimized seed molecule by sampling around the important region, we further considered the synthesizability-unknown seed molecules whose property is already optimized from the previous JT-VAE (Jin et al., 2018) and conditional generative model, SSVAE, (Kang

& Cho, 2018) for plogP and QED trained with a subset of ZINC database (Figure 7c). Our objective in this experiment is to improve further on plogP and QED by sampling around the previously generated optimal (or near-optimal) compounds. As observed, for plogP, our approach could highly improve the property of the seed molecule from 5.30 to 7.37 and from 4.93 to 5.29 (**i** and **ii** in Figure 7c) while ensuring synthesizability based on multi-step reaction sequence. For QED, our model did not improve the property much but still suggested the molecules with plausible synthesis pathways (**iii** and **iv** Figure 7c).

The docking scores of generated compounds as drug candidates against two proteins (i.e. DRD3 (PDB ID: 3PBL) and M^{pro} of SARS-Cov-2 (PDB ID: 7L11)) were also considered for further application of our approach. As seed molecules, we chose the top-scored 200 molecules after calculating docking scores with Quick Vina 2 (Alhossary et al., 2015) among the randomly sampled 5,000 molecules from the ZINC database enumerated from Therapeutic Data Common (TDC) interface (consisting of ∼250,000 molecules) (Huang et al., 2021). We iterated those processes three times independently with different random seed, and we plotted the results obtained from the latter three trials in Figure 8. As shown in Figure 8a and 8b, while both DINGOS-20+ and C-RSVAE generated molecules with higher docking properties than the seed molecules, C-RSVAE performs better than DINGOS-20+ in producing the enhanced docking scores, consistent with other properties shown in Figure 7. Some of the examples (compounds with its synthesis routes) with higher docking scores for each target protein are shown in Figure 8c and 8d.

4.3. Ablation Study

To investigate the effects of conditions on the structure-preserving generations and the method of imposing such conditions, we implemented a few variants of C-RSVAE (see also Appendix E for additional details on implementation) for comparison. The performance was, again, measured by the ratio of data with the Hamming distance of zero in Figure 9. RSVAE is an autoencoder-based approach without conditional embedding (similar to the DoG-AE in Bradshaw et al. (2020)). While we also considered the direct generation of reaction from the seed molecule embedding, u_{seed}, as similarly done in Gao et al. (2021), it was not effectively trained within our model framework. Thus, we considered Zm-RSAE (Z-matched-RSAE) where the encoded latent vector is aligned with the feature vector of the seed molecule (i.e. regression of u_{seed} to z), intending to replace the latent space of autoencoder with the seed molecule-embedding vector (similar to RetroDoG in Bradshaw et al. (2020)). For RSVAE, we randomly generated unique 50,000 reactions (RSVAE) and selected the most similar molecule. To further aid the sampling, we also selected

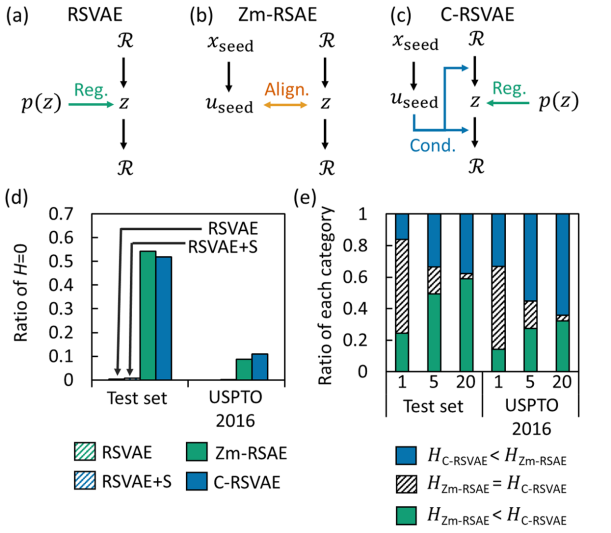

Figure 9. (a-c) Variants of the proposed model used in the ablation study. Green, orange and blue arrows mean the regularization of latent space, alignment of latent vector using target conditions and conditional imposing, respectively. (d) Ratio of generated data with Hamming distance of zero for the structural seed from the test set and USPTO 2016 dataset. (e) Comparison of the top K (=1,5,20) averaged Hamming distance between C-RSVAE and Zm-RSAE.

the starting molecule $m^{(1)}$ using the same hybrid sampling scheme used in C-RSVAE, which we denote as RSVAE+S. In case of Zm-RSAE, we added random Gaussian noise to u_{seed} to generate diverse molecules.

As expected, RSVAE and RSVAE+S could not effectively generate molecules structurally related to the seed molecules due to the lack of proper structural conditioning. Zm-RSAE shows a slightly better generation performance of structurally similar molecules than C-RSVAE for the test set, but for the USPTO 2016 out-of-domain seed molecules, C-RSVAE performs better. The same trend is shown when we take the top K (=1,5,20) averaged Hamming distance values (i.e. $H_{\text{C-RSVAE}}$ and $H_{\text{Zm-RSAE}}$). This differing model performance of Zm-RSAE might be due to the limited generalizability of a neural network for encoding the seed molecule (i.e. f_φ) since f_φ is mainly trained to predict the reaction-embedded latent vector z rather than learning the distribution of reaction representation itself.

5. Conclusion

In this work, we proposed a conditional generative model for generating organic molecules that are structurally similar to the target seed compound while ensuring their synthesizability by predicting the synthesis recipe for the generated molecules. Our model produces synthesis-path-attached "seed-like" molecules by coupling the reaction-embedded

latent vector and seed molecule-embedded conditional vector in the VAE framework. A comparison with a few baseline models demonstrates that utilizing the structural distance of reactants alone is insufficient to generate molecules structurally similar to the seed molecules after applying the chemical reactions, and it is important to incorporate the reaction information in the molecule generation step to preserve the target structural motifs. An encouraging possibility is also shown that our model might be used to design synthetically accessible molecules with even higher chemical activity than the seed molecules optimized from separate molecular design oracles with its synthesizability unknown.

The main limitation of the proposed work for practical use is the fact that the synthesizability of molecules in this work is only defined from the list of pre-defined starting molecules, partner reactants, the number of reaction-steps up to three, and 58 reaction templates. Thus, while a relatively small number of reactions often dominates the overall organic synthesis used in medicinal chemistry (Boström et al., 2018), expanding our model with more diverse reaction templates extracted from existing chemical reactions with either experts' knowledge or data-driven models (Klucznik et al., 2018; Plehiers et al., 2018; Coley et al., 2019; Schwaller et al., 2021; Szymkuć et al., 2021) and reaction data containing longer reaction steps than three as well as the non-linear type of reactions (Bradshaw et al., 2020; Gao et al., 2021) would be needed for generating structurally and synthetically more diverse molecules. For this, the recently proposed local reaction templates (Chen & Jung, 2021) would be helpful to represent diverse reaction types used in drug design by focusing on the local reaction sites. In addition, the current model uses the simple Hamming distance with MACCS key to measure the whole structural similarity which might miss important structural information with a low structural resolution. Thus, our future work would involve developments of the more advanced structural similarity measuring scheme and molecular representation learning (Liu et al., 2019; Wang et al., 2019; Chithrananda et al., 2020; Wang et al., 2022), with a possibility to focus more on the important core skeletons related to the high functionality rather than imposing conditions on the overall structures when measuring the similarity.

6. Acknowledgements

This work was primarily supported by LG AI Research. Y.J. also acknowledges the support from the Institute of Information & Communications Technology Planning & Evaluation (IITP) grant funded by the Korea government under grant number No. 2021-0-02068 (Artificial Intelligence Innovation Hub).

References

Alhossary, A., Handoko, S. D., Mu, Y., and Kwoh, C.-K. Fast, accurate, and reliable molecular docking with quickvina 2. *Bioinformatics*, 31(13):2214–2216, 2015.

Bender, A. and Glen, R. C. Molecular similarity: a key technique in molecular informatics. *Organic & Biomolecular Chemistry*, 2(22):3204–3218, 2004.

Boda, K., Seidel, T., and Gasteiger, J. Structure and reaction based evaluation of synthetic accessibility. *Journal of Computer-Aided Molecular Design*, 21(6):311–325, 2007.

Boström, J., Brown, D. G., Young, R. J., and Keserü, G. M. Expanding the medicinal chemistry synthetic toolbox. *Nature Reviews Drug Discovery*, 17(10):709–727, 2018.

Bradshaw, J., Paige, B., Kusner, M. J., Segler, M., and Hernández-Lobato, J. M. A model to search for synthesizable molecules. *Advances in Neural Information Processing Systems*, 32, 2019.

Bradshaw, J., Paige, B., Kusner, M. J., Segler, M., and Hernández-Lobato, J. M. Barking up the right tree: an approach to search over molecule synthesis dags. *Advances in Neural Information Processing Systems*, 33: 6852–6866, 2020.

Button, A., Merk, D., Hiss, J. A., and Schneider, G. Automated de novo molecular design by hybrid machine intelligence and rule-driven chemical synthesis. *Nature Machine Intelligence*, 1(7):307–315, 2019.

Chen, S. and Jung, Y. Deep retrosynthetic reaction prediction using local reactivity and global attention. *JACS Au*, 1(10):1612–1620, 2021.

Chithrananda, S., Grand, G., and Ramsundar, B. Chemberta: large-scale self-supervised pretraining for molecular property prediction. *arXiv preprint arXiv:2010.09885*, 2020.

Cho, K., Van Merriënboer, B., Bahdanau, D., and Bengio, Y. On the properties of neural machine translation: Encoder-decoder approaches. *arXiv preprint arXiv:1409.1259*, 2014.

Coley, C. W., Rogers, L., Green, W. H., and Jensen, K. F. Computer-assisted retrosynthesis based on molecular similarity. *ACS Central Science*, 3(12):1237–1245, 2017.

Coley, C. W., Green, W. H., and Jensen, K. F. Rdchiral: An rdkit wrapper for handling stereochemistry in retrosynthetic template extraction and application. *Journal of chemical information and modeling*, 59(6):2529–2537, 2019.

Dai, H., Li, C., Coley, C., Dai, B., and Song, L. Retrosynthesis prediction with conditional graph logic network. *Advances in Neural Information Processing Systems*, 32, 2019.

Dai Nguyen, H. and Tsuda, K. A generative model for molecule generation based on chemical reaction trees. *arXiv e-prints*, pp. arXiv–2106, 2021.

Duan, H., Wang, L., Zhang, C., Guo, L., and Li, J. Retrosynthesis with attention-based nmt model and chemical analysis of "wrong" predictions. *RSC Advances*, 10(3): 1371–1378, 2020.

Eckert, H. and Bajorath, J. Molecular similarity analysis in virtual screening: foundations, limitations and novel approaches. *Drug Discovery Today*, 12(5-6):225–233, 2007.

Elton, D. C., Boukouvalas, Z., Fuge, M. D., and Chung, P. W. Deep learning for molecular design—a review of the state of the art. *Molecular Systems Design & Engineering*, 4 (4):828–849, 2019.

Ertl, P. and Schuffenhauer, A. Estimation of synthetic accessibility score of drug-like molecules based on molecular complexity and fragment contributions. *Journal of Cheminformatics*, 1(1):1–11, 2009.

Fu, H., Li, C., Liu, X., Gao, J., Celikyilmaz, A., and Carin, L. Cyclical annealing schedule: A simple approach to mitigating kl vanishing. *arXiv preprint arXiv:1903.10145*, 2019.

Gao, W. and Coley, C. W. The synthesizability of molecules proposed by generative models. *Journal of Chemical Information and Modeling*, 60(12):5714–5723, 2020.

Gao, W., Mercado, R., and Coley, C. W. Amortized tree generation for bottom-up synthesis planning and synthesizable molecular design. *arXiv preprint arXiv:2110.06389*, 2021.

Gómez-Bombarelli, R., Wei, J. N., Duvenaud, D., Hernández-Lobato, J. M., Sánchez-Lengeling, B., Sheberla, D., Aguilera-Iparraguirre, J., Hirzel, T. D., Adams, R. P., and Aspuru-Guzik, A. Automatic chemical design using a data-driven continuous representation of molecules. *ACS Central Science*, 4(2):268–276, 2018.

Gottipati, S. K., Sattarov, B., Niu, S., Pathak, Y., Wei, H., Liu, S., Blackburn, S., Thomas, K., Coley, C., Tang, J., et al. Learning to navigate the synthetically accessible chemical space using reinforcement learning. In *International Conference on Machine Learning*, pp. 3668–3679. PMLR, 2020.

Hartenfeller, M., Eberle, M., Meier, P., Nieto-Oberhuber, C., Altmann, K.-H., Schneider, G., Jacoby, E., and Renner, S. A collection of robust organic synthesis reactions for in silico molecule design. *Journal of Chemical Information and Modeling*, 51(12):3093–3098, 2011.

Hong, S. H., Ryu, S., Lim, J., and Kim, W. Y. Molecular generative model based on an adversarially regularized autoencoder. *Journal of Chemical Information and Modeling*, 60(1):29–36, 2019.

Huang, K., Fu, T., Gao, W., Zhao, Y., Roohani, Y., Leskovec, J., Coley, C. W., Xiao, C., Sun, J., and Zitnik, M. Therapeutics data commons: Machine learning datasets and tasks for drug discovery and development. *arXiv preprint arXiv:2102.09548*, 2021.

Huang, Q., Li, L.-L., and Yang, S.-Y. Rasa: a rapid retrosynthesis-based scoring method for the assessment of synthetic accessibility of drug-like molecules. *Journal of Computer-Aided Molecular Design*, 51(10):2768–2777, 2011.

Jin, W., Barzilay, R., and Jaakkola, T. Junction tree variational autoencoder for molecular graph generation. In *International Conference on Machine Learning*, pp. 2323–2332. PMLR, 2018.

Kang, S. and Cho, K. Conditional molecular design with deep generative models. *Journal of Chemical Information and Modeling*, 59(1):43–52, 2018.

Karpov, P., Godin, G., and Tetko, I. V. A transformer model for retrosynthesis. In *International Conference on Artificial Neural Networks*, pp. 817–830. Springer, 2019.

Kingma, D. P. and Ba, J. Adam: A method for stochastic optimization. *arXiv preprint arXiv:1412.6980*, 2014.

Kingma, D. P. and Welling, M. Auto-encoding variational bayes. *arXiv preprint arXiv:1312.6114*, 2013.

Klucznik, T., Mikulak-Klucznik, B., McCormack, M. P., Lima, H., Szymkuć, S., Bhowmick, M., Molga, K., Zhou, Y., Rickershauser, L., Gajewska, E. P., et al. Efficient syntheses of diverse, medicinally relevant targets planned by computer and executed in the laboratory. *Chem*, 4(3): 522–532, 2018.

Landrum, G. Rdkit: A software suite for cheminformatics, computational chemistry, and predictive modeling, 2013.

Liu, B., Ramsundar, B., Kawthekar, P., Shi, J., Gomes, J., Luu Nguyen, Q., Ho, S., Sloane, J., Wender, P., and Pande, V. Retrosynthetic reaction prediction using neural sequence-to-sequence models. *ACS Central Science*, 3 (10):1103–1113, 2017.

Liu, C.-H., Korablyov, M., Jastrzębski, S., Włodarczyk-Pruszyński, P., Bengio, Y., and Segler, M. H. Retrognn: Approximating retrosynthesis by graph neural networks for de novo drug design. *arXiv preprint arXiv:2011.13042*, 2020.

Liu, S., Demirel, M. F., and Liang, Y. N-gram graph: Simple unsupervised representation for graphs, with applications to molecules. *Advances in Neural Information Processing Systems*, 32, 2019.

Mann, V. and Venkatasubramanian, V. Retrosynthesis prediction using grammar-based neural machine translation: An information-theoretic approach. *Computers & Chemical Engineering*, 155:107533, 2021.

Maziarka, Ł., Pocha, A., Kaczmarczyk, J., Rataj, K., Danel, T., and Warchoł, M. Mol-cyclegan: a generative model for molecular optimization. *Journal of Cheminformatics*, 12(1):1–18, 2020.

Méndez-Lucio, O., Baillif, B., Clevert, D.-A., Rouquié, D., and Wichard, J. De novo generation of hit-like molecules from gene expression signatures using artificial intelligence. *Nature Communications*, 11(1):1–10, 2020.

Nigam, A., Pollice, R., Krenn, M., dos Passos Gomes, G., and Aspuru-Guzik, A. Beyond generative models: superfast traversal, optimization, novelty, exploration and discovery (stoned) algorithm for molecules using selfies. *Chemical Science*, 2021.

Paszke, A., Gross, S., Massa, F., Lerer, A., Bradbury, J., Chanan, G., Killeen, T., Lin, Z., Gimelshein, N., Antiga, L., et al. Pytorch: An imperative style, high-performance deep learning library. *Advances in Neural Information Processing Systems*, 32:8026–8037, 2019.

Plehiers, P. P., Marin, G. B., Stevens, C. V., and Van Geem, K. M. Automated reaction database and reaction network analysis: extraction of reaction templates using cheminformatics. *Journal of Cheminformatics*, 10(1):1–18, 2018.

Pollice, R., dos Passos Gomes, G., Aldeghi, M., Hickman, R. J., Krenn, M., Lavigne, C., Lindner-D'Addario, M., Nigam, A., Ser, C. T., Yao, Z., et al. Data-driven strategies for accelerated materials design. *Accounts of Chemical Research*, 54(4):849–860, 2021.

Putin, E., Asadulaev, A., Ivanenkov, Y., Aladinskiy, V., Sanchez-Lengeling, B., Aspuru-Guzik, A., and Zhavoronkov, A. Reinforced adversarial neural computer for de novo molecular design. *Journal of Chemical Information and Modeling*, 58(6):1194–1204, 2018.

Sacha, M., Błaz, M., Byrski, P., Dabrowski-Tumanski, P., Chrominski, M., Loska, R., Włodarczyk-Pruszynski, P., and Jastrzebski, S. Molecule edit graph attention network: modeling chemical reactions as sequences of graph edits. *Journal of Chemical Information and Modeling*, 61(7): 3273–3284, 2021.

Sanchez-Lengeling, B. and Aspuru-Guzik, A. Inverse molecular design using machine learning: Generative models for matter engineering. *Science*, 361(6400):360–365, 2018.

Schuster, M. and Paliwal, K. K. Bidirectional recurrent neural networks. *IEEE transactions on Signal Processing*, 45(11):2673–2681, 1997.

Schwaller, P., Laino, T., Gaudin, T., Bolgar, P., Hunter, C. A., Bekas, C., and Lee, A. A. Molecular transformer: a model for uncertainty-calibrated chemical reaction prediction. *ACS Central Science*, 5(9):1572–1583, 2019.

Schwaller, P., Petraglia, R., Zullo, V., Nair, V. H., Haeuselmann, R. A., Pisoni, R., Bekas, C., Iuliano, A., and Laino, T. Predicting retrosynthetic pathways using transformer-based models and a hyper-graph exploration strategy. *Chemical Science*, 11(12):3316–3325, 2020.

Schwaller, P., Hoover, B., Reymond, J.-L., Strobelt, H., and Laino, T. Extraction of organic chemistry grammar from unsupervised learning of chemical reactions. *Science Advances*, 7(15):eabe4166, 2021.

Segler, M. H. and Waller, M. P. Neural-symbolic machine learning for retrosynthesis and reaction prediction. *Chemistry–A European Journal*, 23(25):5966–5971, 2017.

Segler, M. H., Preuss, M., and Waller, M. P. Planning chemical syntheses with deep neural networks and symbolic ai. *Nature*, 555(7698):604–610, 2018.

Shi, C., Xu, M., Guo, H., Zhang, M., and Tang, J. A graph to graphs framework for retrosynthesis prediction. In *International Conference on Machine Learning*, pp. 8818–8827. PMLR, 2020.

Sohn, K., Lee, H., and Yan, X. Learning structured output representation using deep conditional generative models. *Advances in Neural Information Processing Systems*, 28, 2015.

Somnath, V. R., Bunne, C., Coley, C., Krause, A., and Barzilay, R. Learning graph models for retrosynthesis prediction. *Advances in Neural Information Processing Systems*, 34:9405–9415, 2021.

Szymkuć, S., Badowski, T., and Grzybowski, B. A. Is organic chemistry really growing exponentially? *Angewandte Chemie*, 133(50):26430–26436, 2021.

Tetko, I. V., Karpov, P., Van Deursen, R., and Godin, G. State-of-the-art augmented nlp transformer models for direct and single-step retrosynthesis. *Nature Communications*, 11(1):1–11, 2020.

Thakkar, A., Chadimova, V., Bjerrum, E. J., Engkvist, O., and Reymond, J.-L. Retrosynthetic accessibility score (rascore)–rapid machine learned synthesizability classification from ai driven retrosynthetic planning. *Chemical Science*, 12(9):3339–3349, 2021.

Ucak, U. V., Ashyrmamatov, I., Ko, J., and Lee, J. Retrosynthetic reaction pathway prediction through neural machine translation of atomic environments. *Nature Communications*, 13(1):1–10, 2022.

Voršilák, M., Kolář, M., Čmelo, I., and Svozil, D. Syba: Bayesian estimation of synthetic accessibility of organic compounds. *Journal of Cheminformatics*, 12:1–13, 2020.

Wang, S., Guo, Y., Wang, Y., Sun, H., and Huang, J. Smiles-bert: large scale unsupervised pre-training for molecular property prediction. In *Proceedings of the 10th ACM international conference on bioinformatics, computational biology and health informatics*, pp. 429–436, 2019.

Wang, Y., Wang, J., Cao, Z., and Barati Farimani, A. Molecular contrastive learning of representations via graph neural networks. *Nature Machine Intelligence*, 4(3):279–287, 2022.

Zunger, A. Inverse design in search of materials with target functionalities. *Nature Reviews Chemistry*, 2(4):1–16, 2018.

A. Model Configurations

Seed Molecule Encoder. Encoding of the target structural template through f_φ is consisting of four-hidden-layer MLP with hidden layer dimension of 200, and ReLU activation function is used. The output of f_φ (i.e. u_{seed}) is normalized by its magnitude to ensure that any given condition is on the same hypersphere with radius of 1.

Reaction Sequence Encoder. Reaction sequence encoder q_ϕ is consisting of two-stacked bi-directional GRU (Schuster & Paliwal, 1997; Cho et al., 2014) with the hidden state dimension of 512, and the initial state is set to zero. $x_m^{(i)}$ and $x_p^{(i)}$ are embedded using a linear layer with dimension of 256. F_h, an MLP for computing μ and σ, is consisting of two-hidden-layer MLP with ReLU activation function, and the dimension of hidden layer is 512. The dimension of latent vector z is 200.

Decoder. Both p_{θ_t} and p_{θ_r} are consisting of two-stacked uni-directional GRU, and the dimension of hidden state is 512. Initial state of each GRU is obtained from the linear layer which takes z and u_{seed} as input. $x_m^{(i)}$ is embedded through a linear layer with dimension of 256. F_t and F_r are consisting of two-hidden-layer MLP with the hidden layer dimension of 512, and ReLU activation function is used.

B. Model Training and Molecule Database

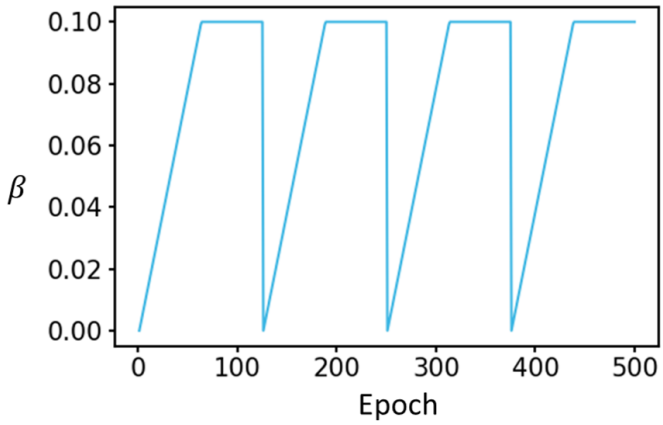

Figure 10. Scheduling of cyclic annealing of β for regularization of the latent space using KL-divergence.

Training of C-RSVAE. For the model training, we empirically set the hyperparameters. In detail, we used $\alpha = 0.3$, and applied cyclic annealing (Fu et al., 2019) for KL-divergence term by changing the value of β from 0 to 0.1. All of the parameters used in cyclic annealing are default values of the original work (Fu et al., 2019). In detail, we set the number of cycles as 4 (i.e. repeating four times of annealing) during training epoch of 500. For each cycle, the value of β is increased linearly during the initial 50 % of a cycle, and fixed it to be a maximum value of 0.1 during the remain 50 % of a cycle (Figure 10). For optimization of model parameters, we randomly sampled 2 M of reaction sequences for model training 95 %) and validation (5 %) among the total 3 M reaction sequences. All the parameters in encoder and decoder are jointly optimized using the Adam optimizer (Kingma & Ba, 2014) with a learning rate of 0.00005.

Molecule Database. For molecule database, we used 150,560 commercially available molecules obtained from Gottipati et al. (2020) and additionally filtered the molecules using the molecular weight (in g/mol) condition (i.e. range of [100, 300]) yielding a total 137,687 molecules ($\sim$ 91 % of total available molecules). Here, we randomly sampled 5,000 from the previously constructed 137,687 molecules set, and defined it as a library of the starting molecules $\mathcal{M}$. Also, all the 137,687 molecules are used as the library of the partner reactants $\mathcal{P}$.

C. Partner Reactant Prediction in DINGOS

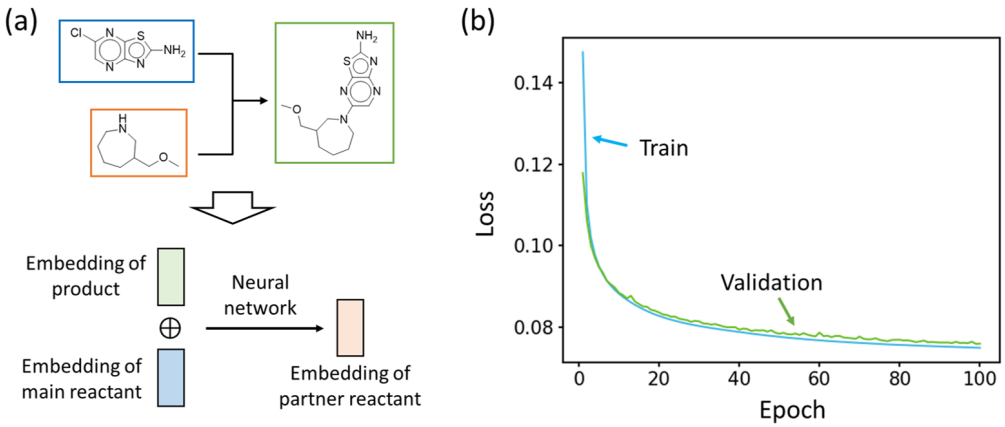

Figure 11. (a) Schematic diagram of neural network model used in DINGOS. (b) Loss trajectory for ML used in DINGOS.

For sampling with DINGOS, we trained a neural network (NN) predicting the embedding of partner reactant from the embedding of product and main reactant as shown in Figure 11a (Button et al., 2019). For NN, we used single linear layer with dimension of 334 followed by sigmoid activation function, and binary cross entropy loss is used for model training (epoch size = 100, see Figure 11b for loss trajectory). All the molecules are embedded with MACCS key. For dataset, we decomposed all 3 M reactions into the one-step reactions, and removed the duplicates yielding a total 5,635,419 unique reactions. We randomly sampled 2 M reactions from the latter obtained unique one-step reactions for model construction (train/validation = 95/5 %). When utilizing the trained model for sampling new reactions, embedding of the product is replaced by the embedding of seed molecule (Button et al., 2019).

D. Implementation Details on Reaction Sampling

Sampling with Generative Model. For sampling of reaction sequences with the trained generative model, we sampled 200 latent vectors from the normal distribution with a fixed random seed. For sampling with each latent vector, we set $k = 20$ for k-nearest-neighbor sampling for the selection of starting molecule ($m^{(1)}$), and set $k = 1$ for sampling of the partner reactant ($p^{(i)}$). We set the maximum number of reaction step as 3 (i.e. $n_{\max} = 3$), and rejected the reactions if the Hamming distance value increases compared to the previous step (i.e. $H_{\text{most-recent}} > H_{\text{previous-step}}$) (Button et al., 2019).

Sampling with DINGOS-*k*. We sampled k starting molecules $m^{(1)}$ using the Hamming distance between the seed molecule and molecules in the pre-defined set of starting molecules $\mathcal{M}$. Partner reactant $p^{(i)}$ is sampled through the K-nearest-neighbor sampling with the Hamming distance between the pre-defined set of partner reactants $\mathcal{P}$ and the output of trained NN as shown in Appendix C. Here, we set $k = 20$ for sampling $p^{(i)}$. We set the maximum number of reaction step as 3 (i.e. $n_{\max} = 3$), and also set the cut-off value of molecular weight as 1.5 times of the molecular weight of the target condition. Furthermore, we rejected reactions if the Hamming distance value increases compared to the previous step (i.e. $n_{\max} = 3$), and rejected the reactions if the Hamming distance value increases compared to the previous step (i.e. $H_{\text{most-recent}} > H_{\text{previous-step}}$) (Button et al., 2019).

E. Implementation Details of Models used in Ablation Study

RSVAE. We excluded any information related to the target seed molecule. Thus, the latent vector is obtained using reparameterization trick as following:

$$[\mu, \sigma] = F_h(\text{BiGRU}([x_r^{(1)}, x_r^{(2)}, ..., x_r^{(L)}])) \tag{10}$$

$$\tag{11}$$

Reaction templates and pair reactants are obtained from z as following, and we used same training scheme as done in C-RSVAE.

$$\hat{x}_t^{(j)} \sim p_{\theta_t}(m^{(j)}|z) = \text{Softmax}[F_t(\text{GRU}(x_m^{(j)}|z))] \tag{12}$$

$$\hat{x}_p^{(k)} \sim p_{\theta_r}(m^{(k)}, t^{(k)}|z) = \text{Softmax}[F_t(\text{GRU}([x_m^{(k)} \oplus x_t^{(k)}]|z))] \tag{13}$$

where $j \in [1, L]$ and $k \in [0, L-1]$.

Zm-RSAE. The latent vector is directly computed from encoder without reparameterization trick used in the conventional VAE. That is,

$$z = F_h(\text{BiGRU}([x_r^{(1)}, x_r^{(2)}, ..., x_r^{(L)}])) \tag{14}$$

For alignment of latent vector, we used mean-squared error term for latent space alignment (i.e. $\parallel u_{\text{seed}} - z \parallel_2^2$) without KL-divergence term. We added random Gaussian noise to each encoded feature (i.e. u_{seed} and z) during training, and trained Zm-RSAE during 200 epochs.

Selecting Starting Molecules with RSVAE and Zm-RSAE. For selecting of starting molecules with RSVAE and Zm-RSAE as used in ablation study, we used following *k*-nearest-neighbor sampling scheme:

$$[m_1^{(1)}, ..., m_k^{(1)}]_{\text{RSVAE}} \sim k\text{NN}_{m \in \mathcal{M}}[H(\hat{x}_m^{(1)}, x_m)], \hat{x}_m^{(1)} \sim p_{\theta_r}^{\text{RSVAE}}(m^{(0)}, t^{(0)}|z) \tag{15}$$

$$[m_1^{(1)}, ..., m_k^{(1)}]_{\text{RSVAE+S}} \sim k\text{NN}_{m \in \mathcal{M}}[H(\hat{x}_m^{(1)}, x_m) + H(x_{\text{seed}}, x_m)], \hat{x}_m^{(1)} \sim p_{\theta_r}^{\text{RSVAE}}(m^{(0)}, t^{(0)}|z) \tag{16}$$

$$[m_1^{(1)}, ..., m_k^{(1)}]_{\text{Zm-RSAE}} \sim k\text{NN}_{m \in \mathcal{M}}[H(\hat{x}_m^{(1)}, x_m)], \hat{x}_m^{(1)} \sim p_{\theta_r}^{\text{Zm-RSAE}}(m^{(0)}, t^{(0)}|u_{\text{seed}}) \tag{17}$$

F. Sampling Reactions by Changing Mixing Parameter, λ

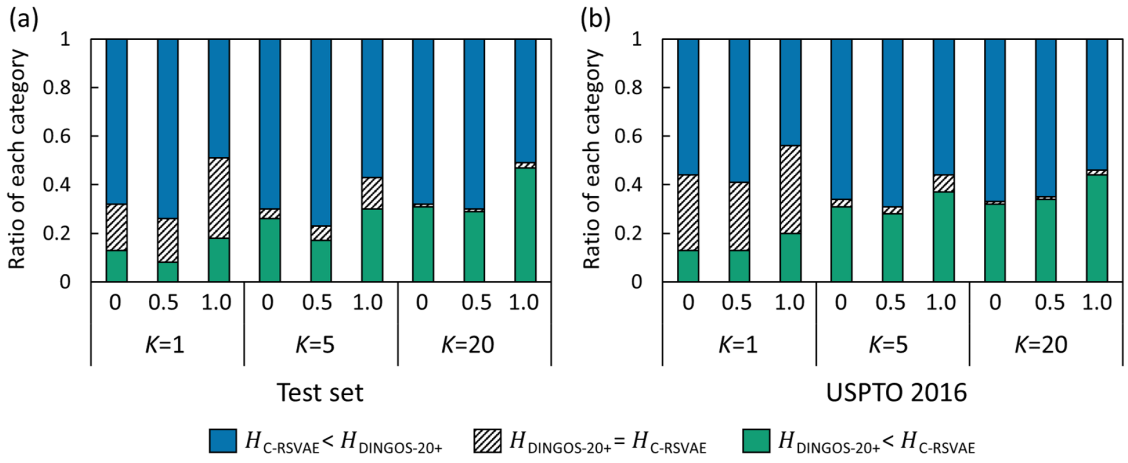

Figure 12. Comparison of the top K (=1,5,20) averaged Hamming distance between C-RSVAE and DINGOS by changing the mixing parameter λ for the seed molecules sampled from (a) test set and (b) USPTO 2016 data.

We investigated the performance of C-RSVAE for generating molecules with three different λ values (i.e. 0, 0.5 and 1.0). For this experiment, 100 seed molecules are chosen from the test set and USPTO 2016. We compared the top K averaged Hamming distance for the molecules generated from each approach (i.e. C-RSVAE and DINGOS-20+). As shown in Figure 12, we decomposed the seed molecules into three categories as done in Figure 5 in main text. As observed, even for the case of $\lambda = 0$, the proposed C-RSVAE could generate molecules more similar to the desired seed molecules than DINGOS-20+ (i.e. $67 \sim 70$ % for test set and $56 \sim 67$ % for USPTO 2016). In addition, our model still outperforms DINGOS-20+ when the same type of starting reactants is used (see results with $\lambda = 1.0$), indicating the effectiveness of utilizing reaction-embedded latent vector for sampling new molecules structurally similar to the target seed molecule. Notably, sampling with $\lambda = 0.5$, corresponding to our proposed approach, shows the best performance compared to the other cases (i.e. $70 \sim 77$ % for test set and $59 \sim 68$ % for USPTO 2016).

G. A Preliminary Comparison with SynNet

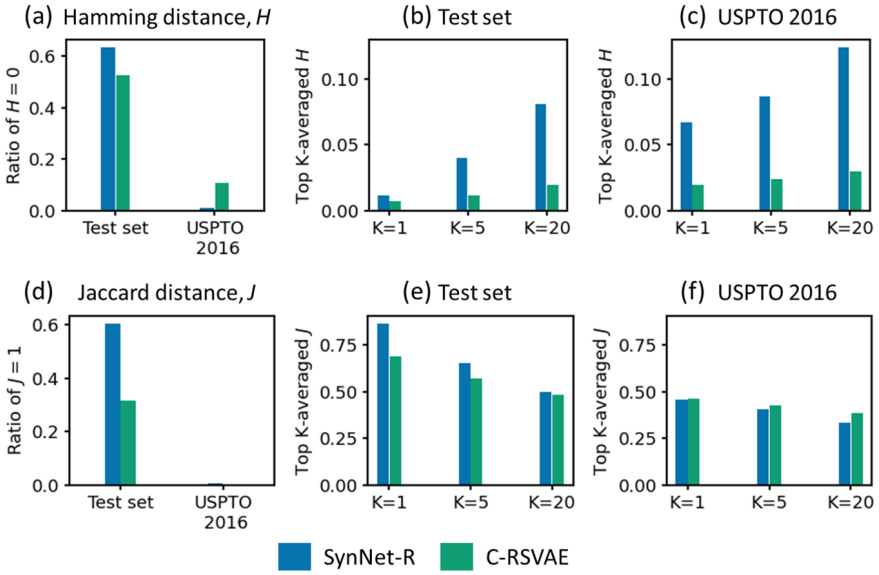

Figure 13. The comparison of C-RSVAE and SynNet-R for the similarity of the generated molecules. The reconstruction ratio of the generated data with (a) Hamming distance of 0 (i.e. $H = 0$) and (d) Jaccard distance of 1 (i.e. $J = 1$) for the target seed molecules randomly chosen from the test set and USPTO 2016. The (b-c) average Hamming or (e-f) average Jaccard distances for the top K (=1,5,20) similar molecules generated using C-RSVAE and SynNet-R.

In addition to the ablation study with the straightforward variants of our model as described in the main text, a brief further comparative experiment with a direct conditional approach (SynNet) by Gao et al. (2021) is performed. We retrained the SynNet with the same training data used in this work, denoted in Figure 13 as SynNet-R. We randomly sampled 550,000 reactions from our original training data and applied the QED filters for the final product of each reaction in the dataset, following Gao et al. (2021). This yielded 348,627 reactions included for the training of SynNet-R. For sampling of reactions with SynNet-R, 30 most similar starting molecules are selected based on the Hamming distance (i.e. H, Figure 13a-c) or Jaccard distance (i.e. J, Figure 13d-f), and we ensured that more than 20 unique reactions were obtained from this. We used 1,000 seed molecules from the test set or USPTO 2016 (same as Figure 4). The results are summarized in Figure 13. The SynNet's reconstruction accuracy is higher than that of C-RSVAE for the test set seed molecules on both the similarity metrics, but for the out-of-domain USPTO-2016, the C-RSVAE's reconstruction performance is slightly higher than that of SynNet on the Hamming distance or comparable to it on the Jaccard distance (Figure 13a and d). Very small reconstruction ratios for both C-RSVAE and SynNet on the Jaccard distance are due to the limited reaction templates and starting molecules used in this work which cannot treat the out of domain USPTO reactions (Figure 13d). This should be improved using the larger set of templates and starting molecules. A similar trend is shown when considering the average Hamming or Jaccard distances of the top-K similar molecules (overall similarity distribution, Figure 13b-c, and 13e-f). On the Hamming distance, C-RSVAE yields on average more similar molecules for all K on both the test and USPTO molecules, but on the average Jaccard distances, for all K, the in-domain test set performance is better in SynNet while the out-of-domain USPTO performance is slightly better in C-RSVAE. Thus, while a more systematic comparison through further optimization and more advanced schemes for molecular representation learning and similarity evaluation would be required, these results suggest that the joint learning of the reaction and the target seed molecular space can be a competitive approach to sample diverse synthesizable molecules imposed to have a structural similarity.